CHINESE OPTICS LETTERS

Vol. 20, No. 1 | January 2022

Theoretical and experimental analysis of second order Bragg resonance of 45° TFG and its fiber laser application

Qingguo Song (宋青果)[1], Bolin Ye (叶柏林)[2], Xiangpeng Xiao (肖翔鹏)[1], Chengjun Huang (黄成俊)[1], Chengbo Mou (牟成博)[3], Zhijun Yan (闫志君)[1*], and Lin Zhang (张 琳)[4]

[1] School of Optical and Electronic Information, NGIA, Huazhong University of Science and Technology, Wuhan 430074, China

[2] Shenzhen Techwinsemi Optoelectronic Co., Ltd., Shenzhen 518000, China

[3] Key Laboratory of Specialty Fiber Optics and Optical Access Networks, Shanghai Institute for Advanced Communication and Data Science, Joint International Research Laboratory of Specialty Fiber Optics and Advanced Communication, Shanghai University, Shanghai 200444, China

[4] Aston Institute of Photonic Technologies, Aston University, Birmingham B4 7ET, UK

*Corresponding author: yanzhijun@gmail.com

Received May 11, 2021 | Accepted July 30, 2021 | Posted Online September 28, 2021

We report the observation of second order Bragg resonance (2nd-OBG) produced by tilted fiber gratings (TFGs) fabricated using phase mask UV inscription. The theoretical analysis has revealed that the generation of high order Bragg resonance of gratings is induced by a square-shape refractive index profile, which is caused by over-saturated UV exposure. In the experiment, we have studied the TFGs with different tilt angles under over-saturated UV exposure, in which all gratings have showed the 2nd-OBR, and the larger tilt angle of the grating has the stronger 2nd-OBR. When the tilt angle of the grating is ∼45°, the Bragg resonance exhibits very strong polarization dependence, because the 2nd-OBR wavelength is located within the polarizing bandwidth of 45° TFG. Finally, we have demonstrated an erbium-doped fiber laser with > 99.9% degree of polarization, and, by applying mechanical stretching on the grating, a wavelength tunable laser output has been achieved. The output laser shows ∼0.2 dB amplitude variation within 1 h continuous monitoring of the laser.

Keywords: tilted fiber grating; fiber laser.
DOI: 10.3788/COL202220.012201

1. Introduction

UV-inscribed fiber Bragg gratings (FBGs) are ideal optical devices in telecom, lasers, and sensing systems. The phase mask scanning technique offers high quality FBG fabrication with high reproducibility and ease of design. So far, most of the FBGs reported using a phase mask scanning method are based on the first order Bragg diffraction of the fiber grating structure. It is well known that due to the saturation effect of the UV irradiation, high order Bragg resonance can be observed in a non-tilted uniform FBG[1]. It has been reported that the first and second order Bragg resonances (2nd-OBR) of the same FBG can be used for temperature and strain sensing at the same time[2,3]. Furthermore, an all-fiber spectroscope with a second order FBG for a rotational Raman lidar is reported, in which an all-fiber spectroscopic filter with several second order FBGs and optical fiber couplers is designed based on the narrower reflectivity bandwidth of a second order FBG[4]. So far, all of these reports about high order Bragg resonance are based on a non-tilted uniform FBG. In more recent years, fiber gratings with tilted fringes have attracted a lot of attention. Various tilted structures with small[5], Brewster[6,7], and large[8] angles have been studied. They exhibit excellent performance in sensors[9–11] and in fiber lasers[12–14]. Recently, Zhang *et al.* have reported a high order tilted FBG with superposed refractive index modulation, in which the grating shows two kinds of high order Bragg resonance and cladding mode resonances[15]. Mou *et al.* have observed the 2nd-OBR of a tilted fiber grating (TFG)[16], however, in that Letter, they did not give an explanation of the 2nd-OBR. In this Letter, we systematically analyzed the generation principle of 2nd-OBR of TFGs fabricated and experimentally observed the 2nd-OBR of TFGs with various tilt angles from 0° to 45° fabricated by using UV inscription via a phase mask, in which 2nd-OBR of the 45° TFG has shown very strong polarization dependence. Finally, we have employed the 2nd-OBR of 45° TFG to achieve an all-fiber polarized laser system. In the second part, the application of 2nd-OBR is demonstrated for generating polarized output from a standard ring cavity fiber laser.

2. Theoretical and Experimental Analysis

The Bragg diffraction of a uniform FBG is defined as $\lambda_m = 2n_{\text{eff}} \cdot \Lambda_{\text{axis}}/m$, where λ_m is the mth Bragg resonance wavelength of FBG, m is the diffraction order, n_{eff} is the effective index of the propagating mode, and Λ_{axis} is the axial period of the fiber grating. In general, the grating fringes induced by UV inscription through phase mask have a quasi-ideal sinusoidal refractive index distribution along the fiber axis. However, when the refractive index changes to saturation, which means the fiber has a large UV-exposure dose, the refractive index distribution tends to be square. According to Fourier series analysis, high order frequency components will be generated in the frequency domain, and a series of high order Bragg resonance peaks will appear in the spectrum. For TFGs, the tilted fringes destroy the sinusoidal refractive index distribution along the fiber axis to a greater extent, and the higher order Bragg resonance is easier to obtain.

According to the Kramers–Kronig relationship[17], the refractive index change is generally linearly related to the number of absorption photons and is expressed as

$$\delta n(z) = \delta n_s \cdot \left\{1 - \exp\left\{-\frac{P \cdot t}{2E_s}\left[1 + \nu \cos\left(\frac{\pi z \cos\theta}{\Lambda}\right)\right]\right\}\right\}, \tag{1}$$

where P is the incident optical power, t is the exposure time, ν is the fringe visibility, and θ is the tilted angle of grating. Λ represents the period of the grating. δn_s and E_s represent the saturation index variation and the saturation energy, respectively, which are connected with the core dopant concentration of the photorefractive fiber.

Figure 1(a) shows the simulation result of the normalized index change curve at different UV-exposure time. When the index change gets saturated, the refractive index profile tends to be a square shape, which results in high order Fourier components. The refractive index change can be expanded as a Fourier series, which expressed as

$$\delta n(z) = \delta n_0 + \sum_m \delta n_m \cos\left(\frac{2\pi z \cos\theta}{\Lambda} \cdot m + \varphi_m\right), \tag{2}$$

where δn_0 is the average refractive index change, m is the order number, and φ_m is the phase of the mth order refractive index profile. δn_m is the Fourier series term of the mth order, and it can be expressed as

$$\delta n_m = \frac{2}{\Lambda}\int_0^{\Lambda} \delta n(z) \cdot \cos\left(\frac{2\pi m \cos\theta}{\Lambda}\right) \mathrm{d}z. \tag{3}$$

According to the coupled mode theory, the maximum reflectivity of the mth order can be expressed as

$$R_m = \tan\mathrm{h}^2(\kappa_m \cdot L), \tag{4}$$

where L is the grating length. κ_m is the AC coupling coefficient of the mth order, and it can be expressed as

$$\kappa_m = \Gamma \cdot \delta n_s \cdot \delta n_m, \tag{5}$$

where Γ is the core power confinement factor for the guided mode. In Fig. 1(b), the simulation result shows the reflectivity variation of the first, second, and third orders with the UV-exposure time. The saturation index variation $\delta n_s = 0.001$[18], and the saturation-exposure energy density $E_s = 140\,\mathrm{J/cm^2}$[4]. The first order resonance tends to be saturated at 150 s, corresponding to the rapid increase of the second order resonance. Moreover, the second order resonance tends to be saturated at 1500 s, corresponding to a square refractive index profile. Besides, the third order resonance remains weak over the exposure time. The simulation result clearly shows that with the increase of exposure time, the refractive index distortions of the first and second orders are generated and increased, and that of the third order is hard to observe.

A set of TFGs were UV-inscribed in B/Ge co-doped commercial photosensitive fiber (Fibercore PS1200/1500) using the scanning phase mask technique and a 244 nm UV source from a CW frequency doubled Ar+ laser (Coherent Sabre Fred). The B/Ge fibers were hydrogen-loaded at 150 bar (1 bar = 1×10^5 Pa) at 80°C for two days prior to the UV inscription to further enhance the photosensitivity. The phase mask (IBSEN Photonics) has a uniform period of 1800 nm. The fabrication process of the TFG is given by Ref. [7]. By adjusting the goniometer, we fabricated six TFGs whose angles are 0°, 12.3°, 22°, 30.6°, 36.9°, and 45°, in which the axis periods of the TFG are 900 nm, 908 nm, 932 nm, 967 nm, 1006 nm, and 1080 nm, and the corresponding the wavelengths of 2nd-OBR are 1305 nm, 1318 nm, 1350 nm, 1400 nm, 1460 nm, and 1568 nm, respectively. The grating length is 24 mm. A broadband light source (Agilent 83437 A, range from 1200 nm to 1700 nm) and an optical spectrum analyzer (OSA) were used to monitor the transmission spectra during the grating fabrication. All of the gratings were fabricated under the same UV illumination condition. During the UV-inscription process, the UV laser outputs a 100 mW CW laser with around 500 μm diameter Gaussian beams. For inscription of 45° TFG, the beam size of the laser after the cylindrical lens should be larger than 84 μm[7], which is set around 100 μm at the normal of the fiber axis and 500 μm along the fiber axis. The grating scanning speed is 0.08 mm/s, which corresponds to the exposure time of 1.2 s.

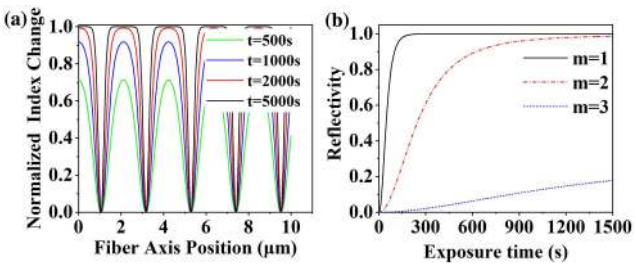

Fig. 1. (a) Simulation of normalized index change at different exposure time; (b) simulation of second order reflectivity against exposure time.

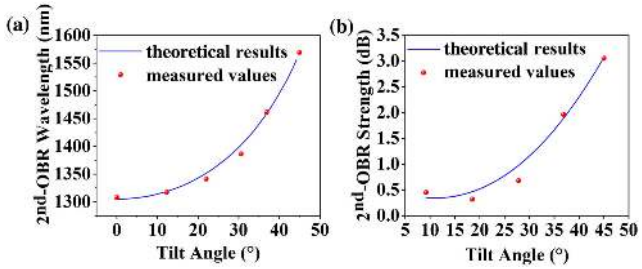

Fig. 2. (a) Experimental and theoretical relationship between the 2nd-OBR wavelength and the grating tilt angle; (b) 2nd-OBR strength against the tilt angle.

The UV dose is defined as $E_{UV} = I_{UV} \cdot t$, where E_{UV} is the UV dose, I_{UV} is the UV intensity, and t is the exposure time. The total UV-exposure dose of TFG in the PS1250/1500 single mode fiber is around 240 J/cm^2. Under such a high UV-exposure dose, the refractive index of the grating would have a square profile.

In Fig. 2(a), the plot depicts the measured 2nd-OBR wavelength of each TFG against the tilt angle. The results show very good accordance with the theoretical simulation. As the angle increases, the resonance wavelength has a corresponding red shift. We also analyzed the grating strength against the tilt angle, which is shown in Fig. 2(b). Under the same UV illumination power and exposure time, it is found that the larger the tilt angle is, the stronger the 2nd-OBR is. At certain angles, especially small angles, multiple scanning may have to be employed to make the 2nd-OBR effect more pronounced. This is because when the grating is slightly tilted, the grating refractive index profile tends to be more sinusoidal, and hence the higher order resonance will not be strong enough to observe.

Previously, it was reported that when the grating tilted angle is 45° during the UV-inscription procedure, the TFG exhibits stronger polarization dependent loss (PDL) over a wide range than other tilted angles[6]. In such a TFG, the p-polarization light is almost lossless, while s-polarization light suffers significant loss, functioning as an in-fiber polarizer. The PDL range of the 45° TFG is around 1400–1700 nm, and only the 2nd-OBR is in this range. We further examined the polarization properties of the 2nd-OBR of the TFG at this particular angle using a set of commercial PDL characterization kits (LUNA Technologies) incorporating an external tunable laser with 20 pm resolution. As expected, we found that the 2nd-OBR of 45° TFG also exhibits large polarization dependency. Figure 3 shows the transmission spectra of the 2nd-OBR generated at 1566.9 nm with a bandwidth of ~0.1 nm. In order to produce a strong 2nd-OBR, we further increase the UV illumination power. The resultant loss of 2nd-OBR is ~12 dB, corresponding to a reflectivity of ~93.7%. This is comparable to the reflectivity of a standard FBG that can be used as reflector in an erbium-doped fiber laser. The PDL resolved spectrum of the 45° TFG shows that the s polarization has a significant loss with a pronounced 2nd–OBR, while p polarization shows only ~0.2 dB insertion loss with a stronger 2nd-OBR. The two 2nd-OBRs locate around slightly different wavelengths (when zoomed in, ~0.02 nm difference in wavelength can be measured) due to the polarization mode dispersion. In addition, typical cladding modes resulting from a standard FBG can be clearly observed on the left side of the Bragg resonance. This further proved the effective generation of a 2nd-OBR.

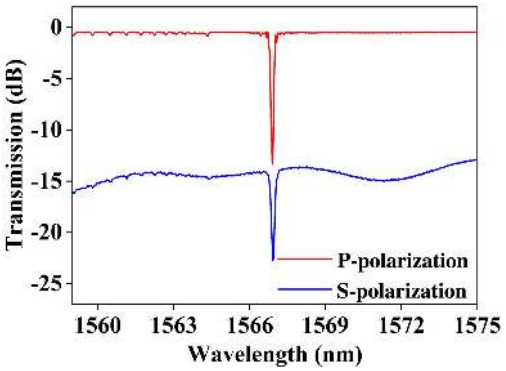

Fig. 3. Measured PDL spectra of the corresponding grating within 30 nm spectrum range showing 2nd-OBR in both p polarization and s polarization.

3. Application of Single Polarization Fiber Laser

Erbium-doped fiber lasers are useful light sources in telecom and sensing systems where single polarization and single wavelength operation is desirable. There are numerous ways to produce polarized output laser. However, they use either expensive specialty fibers[19–21] or high birefringence FBGs[22,23]. Mou has reported the high degree of polarization (DOP) fiber laser system by using an FBG and a 45° TFG, in which the FBG was used for wavelength selection and the 45° TFG introduced a high polarization dependence loss in the laser cavity[24]. In this Letter, we have used the polarization dependent Bragg resonance of the 2nd-OBR of the 45° TFG to achieve a polarized fiber laser system.

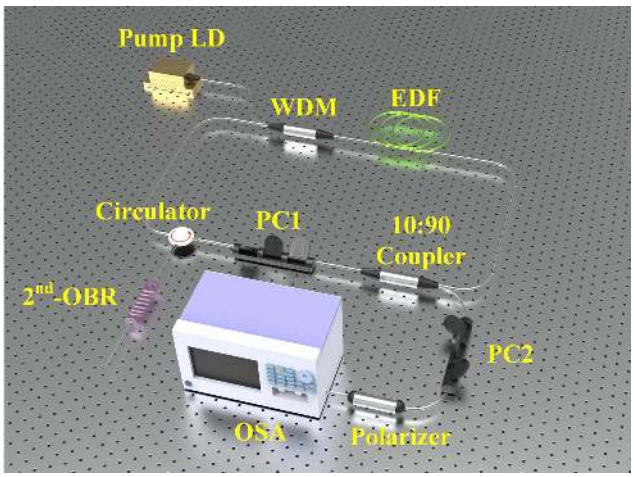

Fig. 4. Schematic of the demonstrated fiber laser using the 2nd-OBR generated by a 45° TFG.

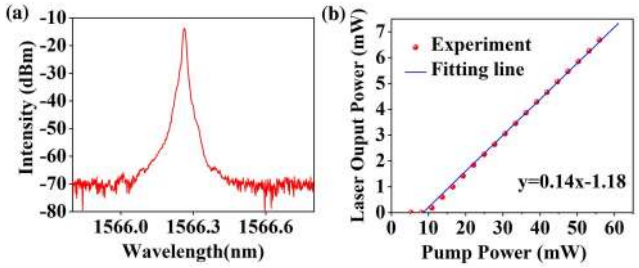

Fig. 5. (a) Typical output spectrum of the fiber laser; (b) slope efficiency of the fiber laser.

The fiber laser construction is shown in Fig. 4, which consists of an ~6 m erbium-doped fiber (Lucent Technologies), a 980 nm/1500 nm wavelength division multiplexer (WDM), a 975 nm laser diode (LD) with up to 300 mW pump power, a fiber polarization controller (PC1) used for cavity optimization, a 10:90 fused coupler for laser output, and a 2nd-OBR grating connected through an optical circulator to provide single wavelength operation. The output spectrum of the fiber laser is measured through an OSA (AQ6370D). Moreover, the polarization extinction ratio (PER) measuring system is constructed by using a fiber PC2, a polarizer, and an OSA. Through adjusting PC2, the spectra of maximal power and minimal power can be obtained, which represent the oscillating p-polarization and s-polarization states, respectively.

The experiment results show that the laser has output a single wavelength laser at ~1566.3 nm with 0.1 nm 3 dB bandwidth and > 50 dB optical signal to noise ratio (OSNR), seen in Fig. 5(a), in which the threshold power and slope efficiency of laser system are ~12 mW and 14%, respectively, seen in Fig. 5(b). Due to the high PDL of Bragg resonance of the 2nd-OBR of 45° TFG, the output laser shows a 33 dB polarization dependent output, which is around 99.9% DOP, seen in Fig. 6(a). By employing strain on the 2nd-OBR, the laser could achieve ~0.4 nm continuous tuning range from 1566.26 nm to 1566.66 nm. The strain sensitivity of the 2nd-OBR is around 1.2 pm/με. Based on the 2000 με strain range of the optical fiber, we could achieve around 2.4 nm wavelength tuning, as shown in Fig. 6(b). The temperature sensitivity of the laser is measured as 0.008 nm/°C, as shown in Fig. 6(c). The experimental results of strain and temperature show that the laser has a good tunability and stability. Furthermore, we also examined the stability of the laser at laboratory conditions for 1 h with 5 min intervals by recording the laser output. The experiment results show ~0.02 nm wavelength variation and only ~0.2 dB output intensity fluence, seen in Fig. 6(d). To obtain a stable laser, temperature and feedback control may be implemented. Here, we would like to show the proof of principle for such a device achieving polarizing light in a fiber laser.

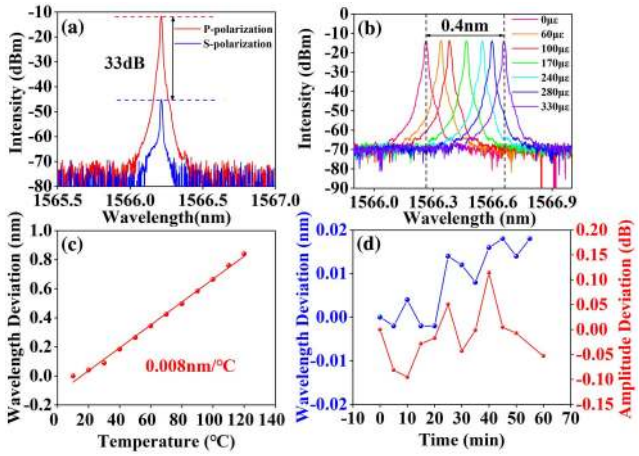

Fig. 6. (a) PER spectra of the laser; (b) tuning ability demonstration of the fiber laser; (c) temperature sensitivity of the fiber laser; (d) output wavelength and amplitude variation of the fiber laser within 1 h in laboratory conditions.

4. Conclusions

In conclusion, we have theoretically and experimentally investigated the 2nd-OBRs of the TFG. Simulation results revealed that the square-shape index modulation profile could enhance the second Bragg resonance of TFG. In the experiment, we have observed the 2nd-OBR of TFG with the tilt angles of 0°, 12.3°, 22°, 30.6°, 36.9°, and 45°. The wavelength of 2nd-OBR of 45° TFG is located just inside of the polarizing bandwidth of 45° TFG, which induces very strong polarization dependent resonance. The 2nd-OBR of 45° TFG would be an ideal polarizing FBG. Based on this, we have achieved a polarized fiber laser system, in which the laser output shows high DOP (> 99.9%), high OSNR (> 50 dB), and capability of continuous tuning with a comparable slope efficiency. The laser showed very stable wavelength and intensity output with ~0.02 nm wavelength variation and ~0.2 dB output intensity fluence. The 2nd-OBR in a TFG would be a simple and effective way to produce a single polarization fiber distributed feedback (DFB) laser.

Acknowledgement

This work was supported in part by the National Natural Science Foundation of China (No. 62075071), the National Science Fund for Excellent Young Scholars (No. 61922033), the '111' Project (No. D20031), and the Shenzhen-Hong Kong Science and Technology Innovation Cooperation Zone applied fundamental research project (No. HZQB-KCZYB-2020082).

References

1. W. X. Xie, M. Douay, P. Bernage, P. Niay, J. F. Bayon, and T. Georges, "Second order diffraction efficiency of Bragg gratings written within germanosilicate fibres," Opt. Commun. **101**, 85 (1993).
2. G. P. Brady, K. Kalli, D. J. Webb, D. Jackson, L. Reekie, and J. L. Archambault, "Simultaneous measurement of strain and temperature using the first and second-order diffraction wavelengths of Bragg gratings," IEE Proc. Optoelectron. **144**, 156 (1997).
3. J. Echevarria, A. Quintela, C. Jauregui, and J. M. López-Higuera, "Uniform fiber Bragg grating first- and second-order diffraction wavelength experimental characterization for strain-temperature discrimination," IEEE Photon. Technol. Lett. **13**, 696 (2001).

4. S. Li, D. Hua, L. Hu, Q. Yan, and X. Tian, "All-fiber spectroscope with second-order fiber Bragg grating for rotational Raman lidar," Spectrosc. Lett. **47**, 244 (2013).
5. J. Albert, L.-Y. Shao, and C. Caucheteur, "Tilted fiber Bragg grating sensors," Laser Photon. Rev. **7**, 83 (2013).
6. X. Guo, Z. Xing, H. Qin, Q. Sun, D. Liu, L. Zhang, and Z. Yan, "Study on polarization spectrum and annealing properties of 45°-tilted fiber gratings," Chin. Opt. Lett. **17**, 050601 (2019).
7. Z. Yan, C. Mou, K. Zhou, X. Chen, and L. Zhang, "UV-inscription, polarization-dependant loss characteristics and applications of 45° tilted fiber gratings," J. Lightwave Technol. **29**, 2715 (2011).
8. Y. Sun, Z. Yan, K. Zhou, B. Luo, B. Jiang, C. Mou, Q. Sun, and L. Zhang, "Excessively tilted fiber grating sensors," J. Lightwave Technol. **39**, 3761 (2021).
9. B. Luo, H. Lu, S. Shi, M. Zhao, J. Lu, Y. Wang, and X. Wang, "Plasmonic gold nanoshell induced spectral effects and refractive index sensing properties of excessively tilted fiber grating," Chin. Opt. Lett. **16**, 100603 (2018).
10. Y. Moreno, Q. Song, Z. Xing, Y. Sun, and Z. Yan, "Hybrid tilted fiber gratings-based surface plasmon resonance sensor and its application for hemoglobin detection," Chin. Opt. Lett. **18**, 100601 (2020).
11. T. Lu, Y. Sun, Y. Moreno, Q. Sun, K. Zhou, H. Wang, Z. Yan, D. Liu, and L. Zhang, "Excessively tilted fiber grating-based vector magnetometer," Opt. Lett. **44**, 2494 (2019).
12. Z. Huang, Q. Huang, A. Theodosiou, X. Cheng, C. Zou, L. Dai, K. Kalli, and C. Mou, "All-fiber passively mode-locked ultrafast laser based on a femtosecond-laser-inscribed in-fiber Brewster device," Opt. Lett. **44**, 5177 (2019).
13. T. Wang, Z. Yan, C. Mou, Z. Liu, Y. Liu, K. Zhou, and L. Zhang, "Narrow bandwidth passively mode locked picosecond erbium doped fiber laser using a 45° tilted fiber grating device," Opt. Express **25**, 16708 (2017).
14. B. Lu, C. Zou, Q. Huang, Z. Yan, Z. Xing, M. Al Araimi, A. Rozhin, K. Zhou, L. Zhang, and C. Mou, "Widely wavelength-tunable mode-locked fiber laser based on a 45°-tilted fiber grating and polarization maintaining fiber," J. Lightwave Technol. **37**, 3571 (2019).
15. X.-Y. Zhang, H.-B. Sun, C. Chen, Y.-S. Yu, W.-H. Wei, Q. Guo, Y.-Y. Chen, X. Zhang, L. Qin, and Y.-Q. Ning, "High-order-tilted fiber Bragg gratings with superposed refractive index modulation," IEEE Photon. J. **10**, 7100308 (2018).
16. C. Mou, R. Suo, K. Zhou, L. Zhang, and I. Bennion, "2nd order Bragg resonance generated in a 45° tilted fiber grating and its application in a fiber laser," in *Advanced Photonics & Renewable Energy, OSA Technical Digest (CD)* (2010), paper BTuA7.
17. T. Erdogan, "Fiber grating spectra," J. Lightwave Technol. **15**, 1277 (1997).
18. Y. D. Gong, T. J. Li, Q. Cai, Q. Li, Z. Wang, Y. L. Guan, J. S. Zhang, and S. S. Jian, "Novel B/Ge codoped photosensitive fiber and dispersion compensation in an 8×10 Gbit/s DWDM system," Opt. Laser Technol. **32**, 23 (2000).
19. M. Kashiwagi, K. Takenaga, K. Ichii, T. Kitabayashi, S. Tanigawa, K. Shima, S. Matsuo, M. Fujimaki, and K. Himeno, "Over 10 W output linearly-polarized single-stage fiber laser oscillating above 1160 nm using Yb-doped polarization-maintaining solid photonic bandgap fiber," IEEE J. Quantum Electron. **47**, 1136 (2011).
20. J. Xu, S. Wu, J. Liu, Y. Li, J. Ren, Q. Yang, and P. Wang, "All-polarization-maintaining femtosecond fiber lasers using graphene oxide saturable absorber," IEEE Photon. Technol. Lett. **26**, 346 (2014).
21. M. S. Astapovich, A. V. Gladyshev, M. M. Khudyakov, A. F. Kosolapov, M. E. Likhachev, and I. A. Bufetov, "Watt-level nanosecond 4.42-μm Raman laser based on silica fiber," IEEE Photon. Technol. Lett. **31**, 78 (2019).
22. D. Pureur, M. Douay, P. Bernage, P. Niay, and J. F. Bayon, "Single-polarization fiber lasers using Bragg gratings in Hi-Bi fibers," J. Lightwave Technol. **13**, 350 (1995).
23. S. Liu, F. Yan, W. Peng, T. Feng, Z. Dong, and G. Chang, "Tunable dual-wavelength thulium-doped fiber laser by employing a HB-FBG," IEEE Photon. Technol. Lett. **26**, 1809 (2014).
24. C. Mou, K. Zhou, L. Zhang, and I. Bennion, "Characterization of 45°-tilted fiber grating and its polarization function in fiber ring laser," J. Opt. Soc. Am. B **26**, 1905 (2009).